Experimental analysis of pressure-discharge relationship in a private water supply tank

Mauro De Marchis, Gabriele Freni and Barbara Milici

ABSTRACT

In Mediterranean countries, users are often equipped with private tanks, which provide a temporary water storage capacity, able to compensate service interruptions due to either scarcity or irregularity of water supply. In the presence of private water storage, water supply is no longer linked to users' consumption and network-operating conditions can be off-design, therefore specific models have to be introduced in simulation models of water distribution networks. Here, a new mathematical model is proposed that is able to reproduce a tank's emptying/filling cycles. Specifically, by means of experimental analysis, a hyperbolic tangent law was tested to reproduce the filling process for private tanks. The flow rate is calculated by means of the classical Torricelli law, in which the float valve emitter coefficient and the valve area are calculated using a function that takes into account the water level within the private tank. The comparison obtained through the mathematical model and those observed from experiments confirmed the ability of the model to predict the flow rate balance within private tanks. The results show that the model is suitable for any length of float valve branch. The mathematical system can be easily used in a transient model to correctly estimate the supplied demand.

Key words | discharge law, experimental pipe network, tank modelling, water distribution network

Mauro De Marchis (corresponding author)
Gabriele Freni
Barbara Milici
Facoltà di Ingegneria, Architettura e Scienze Motorie,
Cittadella Universitaria, Università di Enna 'Kore',
I-94100 Enna,
Italy
E-mail: *mauro.demarchis@unikore.it*

INTRODUCTION

The reliability of water distribution systems is critical for urban activities, because continuous operation of urban water supply has to be ensured at sufficient pressure under different design and operational situations. Models developed for water distribution networks (WDNs) design and management generally take into consideration customer demands as fixed *a priori* outflows concentrated in nodes, independent of nodal heads (demand-driven simulation methods), so they ensure a complete balance between available discharge and required discharge in demand nodes. Under pressure-deficient conditions, head-driven simulation methods, which connect the outflow to the nodal head, are essential for a realistic hydraulic analysis of WDNs.

Head-driven analysis requires the introduction of a nodal outflow discharge model, which links the available discharge to the nodal pressure. Over the past three decades, several authors have derived various relationships, which can be classified into two categories: discontinuous and continuous formulas.

Bhave (1981) was probably the first to introduce the concept of minimum required nodal head value for normal working conditions and suggested a relationship which adopts a [0,1] concept for the head-outflow relationship and admits that full demand is available for heads higher than the minimum required value, whereas there are no discharge results for heads lower than the minimum required value. Germanopoulos (1985) proposed a formula which sets minimum and maximum threshold values such that a constant flow rate is assumed for a nodal head with a higher than maximum required value, zero value is

doi: 10.2166/hydro.2018.135

obtained for pressure with a lower than the minimum threshold value and an exponential law is assumed for an intermediate level of pressure at the node.

Reddy & Elango (1989) suggested outflows wholly dependent on residual heads according to $Q_j = S_j\ (H_j - H_{min})^{0.5}$, where S_j is a node constant, H_j represents the available total head at demand node j and H_{min} represents the pressure head, below which the service at demand node j is unavailable.

Gupta & Bhave (1996) addressed some weaknesses in Germanopoulos's equation and, more recently, several researchers proposed new expressions aimed at improving precision (see Tucciarelli *et al.* 1999; Ackley *et al.* 2001; Tanyimboh *et al.* 2001; Tanyimboh & Templeman 2004, 2010; Tabesh *et al.* 2014; Volpe *et al.* 2014).

However, all these pressure/discharge relationships fail when the service pipe fills a tank which flattens the water demand. Either located on the roof or beneath the ground, private tanks are often considered as very inefficient devices; however, users are often equipped with private tanks because they provide a temporary water storage capacity which is able to compensate possible service interruptions. In fact, either when the network operates under pressure deficient conditions or when water supplies are inadequate to meet consumers' continuous demands – due to either scarcity or irregularity of water resources – discontinuous water distribution and water resources rationing are often used as the main measures to cope with water shortage (De Marchis *et al.* 2011; Freni *et al.* 2014; Puleo *et al.* 2014; Giustolisi *et al.* 2017). In this operative scheme, which is very common all along the Mediterranean coast, users compensate for water service interruptions by collecting water during serviced periods, and delivering it when public water service is not available via gravity or pumping systems, according to the position of the water storage.

Due to filling/emptying cycles, the presence of the tank not only modifies the demand profile of a normal domestic user (with respect to design conditions (Giustolisi *et al.* 2012)) but also makes it impossible to employ classic head/discharge relationships because now the water level in the tank has to be taken into account. In fact, under the assumption that the required nodal pressure is sufficient to supply the tank, the filling process is governed by the action of a proportional float valve that opens partially or completely as a function of the water level in the tank. When the tank is almost full, the water level does not fall enough to induce the valve to open completely, but it dampens the instantaneous water demand and affects the pressure-consumption law. Therefore, in WDNs equipped with private tanks, specific models for the inflow/outflow process of the tank have to be considered; these relationships must be able to correctly estimate the flow rate in two different scenarios. In the former, the tank is not full and the valve is completely open. In this case the discharge is calculated by considering a constant value of the emitter coefficient. In the second case the specific pressure/discharge relationship has to take into account the closure of the orifice at the end of the filling process.

Recently, Giustolisi *et al.* (2014) considered a linear opening of the orifice with volume. However, the orifice feeding inline tanks are controlled by floating valves which do not follow linear behaviour. Therefore, a more accurate discharge law is needed in order to correctly analyse the effect of inline private tanks in WDN models. To this end, Criminisi *et al.* (2009) suggested a model which links the continuity equation for the tank with a float valve emitter law.

De Marchis *et al.* (2016) validated the tank model by Criminisi *et al.* (2009) against experimental data, showing that the model presents some weakness at the start of valve opening and closing.

The experimental research shows the existence of a new mathematical formulation which is able to model the entire experimental data set, obtained by considering three different valve branches. The model can be easily implemented in hydrodynamic models which have to take into account the presence of private tanks, regardless of tank and valve geometry.

MATHEMATICAL SUPPLY MODEL OF INLINE TANKS

This work introduces a pressure-discharge relationship that is able to take into account the presence of local storage. Water tanks are installed to supply water in the event of water shortages or intermittent distribution. The private tanks are usually located on the roof or beneath the ground. This proposed law models the action of the floating

valve during the valve closure period when the valve discharge area progressively decreases as a function of the tank water level.

The model has its origin in the relationship suggested by Criminisi *et al.* (2009), based on the combination of the tank continuity equation:

$$Q_{up} - D = \frac{dV}{dt} = A\frac{dh}{dt} \tag{1}$$

and the float valve emitter law, consistent with the Torricelli law (the kinetic component is considered negligible):

$$Q_{up} = C_v a_v \sqrt{2g(H - z_r)} \tag{2}$$

where D and Q_{up} are the user water demand and the discharge, respectively, and V is the storage volume with area A and variable water depth h. C_v is the float valve emitter coefficient, a_v is the valve discharge area, H is the hydraulic head over the distribution network, z_r is the height of the floating valve and g is the acceleration due to gravity.

The model developed by Criminisi *et al.* (2009) suggested an exponential law in which the float valve emitter coefficient, C_v, depends on the floater position that is on the water level in the tank:

$$C_v = f(h) = \begin{cases} C_v = C_v^* & h \le h_{min} \\ C_v = C_v^* \left(\dfrac{h_{max} - h}{h_{max} - h_{min}}\right)^{\alpha} & h > h_{min} \end{cases} \tag{3}$$

where h_{min} and h_{max} are the water depths when the valve is fully open and fully closed, respectively. C_v^* is the emitter coefficient and α is the exponent and, according to the literature findings, the value ranges between 0.5 and 2, which is experimentally estimated. The emitter coefficient C_v^* spans the interval 0.4–0.8, according to the experiments by Criminisi *et al.* 2009. The same authors also suggested a similar exponential law for the discharge area a_v, as a function of another shape coefficient to be determined experimentally; however, to reduce the number of equations, the discharge area was kept constant and equal to the effective area of the fully-open valve.

As recently observed by De Marchis *et al.* (2016), on the whole the formulation by Criminisi *et al.* (2009) is able to capture the valve-closing phase, but some deviations are observed at the beginning and end of the valve closure.

With the aim of reducing the intrinsic inaccuracy of the float valve model by Criminisi *et al.* (2009), a hyperbolic tangent law for the float valve emitter coefficient C_v is proposed here, which better reproduces the supply system in water tanks, as follows:

$$C_v = f(h) = \begin{cases} C_v = C_v^* & h \le h_{min} \\ C_v = C_v^* tanh\left(m \cdot \dfrac{h_{max} - h}{h_{max} - h_{min}}\right) & h > h_{min} \end{cases} \tag{4}$$

The formulation was obtained through the best fit of the numerical results to a set of laboratory measurements.

Introducing Equation (4) into Equation (2), the following pressure-discharge relationship is obtained:

$$Q_{up} = C_v^* \, tanh\left(m \cdot \frac{h_{max} - h}{h_{max} - h_{min}}\right) a_v \sqrt{2g(H - z_r)} \tag{5}$$

Similarly to Equation (4) for emitter coefficient C_v, a hyperbolic tangent law can be considered for the discharge area a_v, as follows:

$$a_v = g(h) = \begin{cases} a_v = a_v^* & h \le h_{min} \\ a_v = a_v^* \, tanh\left(n \cdot \dfrac{h_{max} - h}{h_{max} - h_{min}}\right) & h > h_{min} \end{cases} \tag{6}$$

Introducing Equations (4) and (6) into Equation (2), the following pressure-discharge relationship holds:

$$Q_{up} = C_v^* a_v^* \tanh\left(m \cdot \frac{h_{max} - h}{h_{max} - h_{min}}\right) \tanh\left(n \cdot \frac{h_{max} - h}{h_{max} - h_{min}}\right) \sqrt{2g(H - z_r)} \tag{7}$$

In Equation (7) the coefficient m is used to calibrate the slope of the hyperbolic tangent law. On the other hand, the coefficient n is the coefficient related to the shape of the float valve area during the closure phase.

EXPERIMENTAL SETUP

Tests were conducted at the Environmental Hydraulic Laboratory of the University of Enna Kore, Italy, where a small WDN reproduced using high-density polyethylene (HDPE 100) pipes of nominal pressure equal to 16 bar (PN16). The WDN has three loops, nine nodes and eleven pipes. All the pipes have the characteristics DN 63 mm, thickness 5.8 mm and approximate length 45 m, and are arranged in horizontal concentric circles with bends, with radius variable in the range of 1.6–2.0 m. This way, a small WDN with three loops was reproduced in actual scale. Figure 1

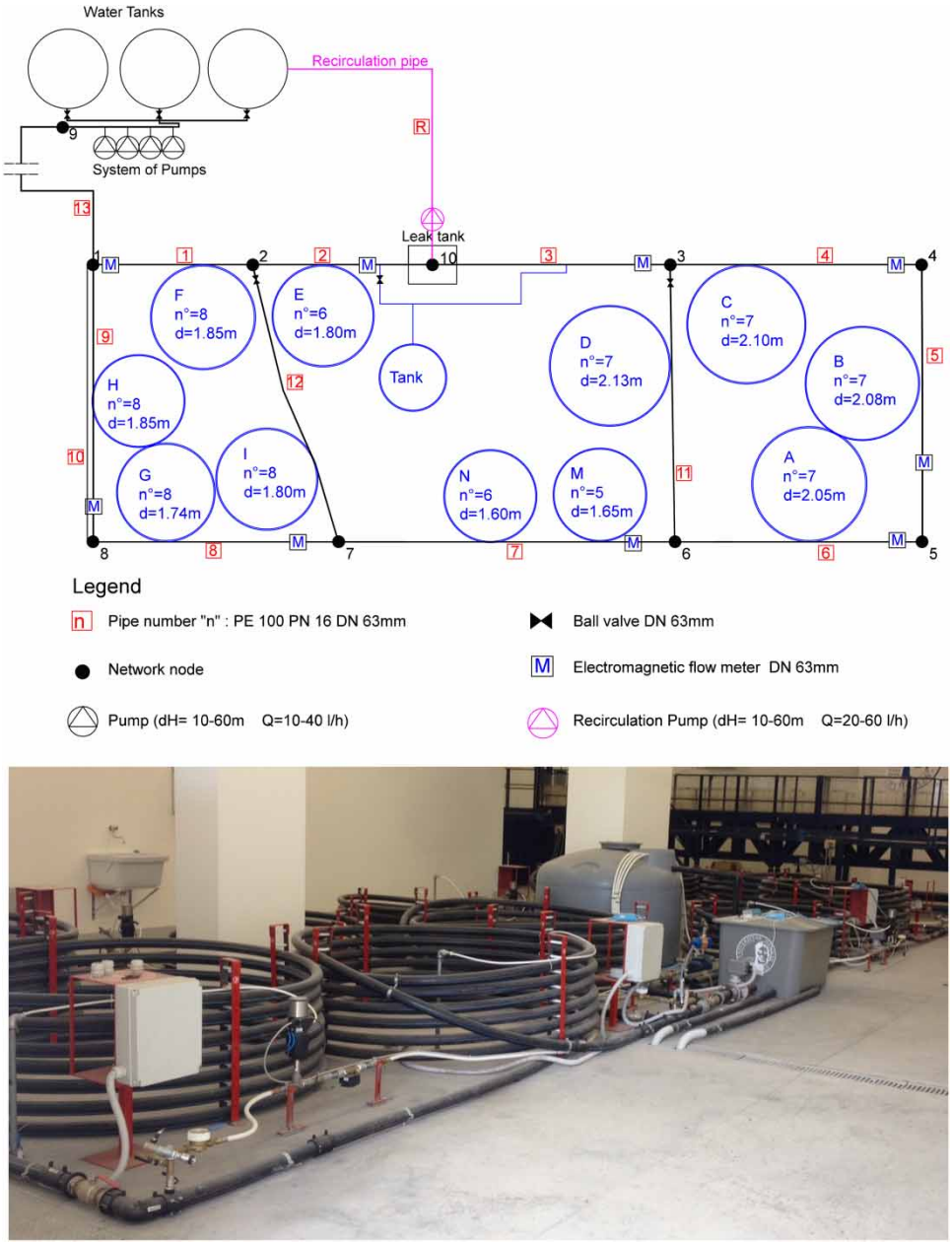

Figure 1 | Top: Layout of the experimental WDN. Bottom: Overview of the WDN.

plots a schematic representation of the WDN and a snapshot of the laboratory.

Four pumps (P) supply the needed discharge from the water tanks to the upstream air vessel (AV) which behaves as a constant head tank, keeping the pressure at the inlet node of the network constant and equal to a prescribed value by varying the speed of the pumps (total water head in the range of 10–60 m). The experimental setup aims at simulating the operational condition of an actual secondary pipe network.

The flow rate is monitored by electromagnetic flow meters, whereas pressure cells are used to measure the water head.

A private tank is located in the roof of the laboratory at approximately 17.5 m above the network level, and it is connected to the system by means of a high-density polyethylene (HDPE 100 PN16) pipe, 30 m long, with a diameter of 12.7 mm. The tank filling process is governed by a float ball valve. Details on the water distribution system can be found in De Marchis *et al.* (2013, 2015a, 2015b, 2016). Here, attention was focused on the filling process of the private tank and especially on the law governing the float valve.

LABORATORY EXPERIMENTS

In the proposed analysis, data collected by De Marchis *et al.* (2016) have been extended, increasing the number of experiments. Specifically, three sets of experiments were carried out by modifying the length of the float valve branch. In the first set of simulations we installed a branch approximately 20 cm long (referred to as test case 1, TC1); in the second set of experiments the float valve was equipped with a branch of 30 cm (referred to as test case 2, TC2). Finally, in the third set of experiments a branch 40 cm long (referred to as test case 3, TC3) was investigated. In Figure 2 a schematic representation of the water tank and float valve relative to the three cases is reported. As shown in the figure, the length of the valve branch affects the water level at which the valve starts to close. In the TC1 the undisturbed water level inside the tank reaches a depth of $h_{min} = 0.60$ cm, whereas when the water depth is $h_{max} = 0.65$ cm the valve can be considered completely closed. On the other hand, in the TC2 the water depth is $h_{min} = 0.56$ cm, and in the TC3 the depth is $h_{min} = 0.53$ cm. In all these cases, the experiments have been carried out considering that at the beginning of each test the water tank was completely empty and is full when the maximum water level is reached and the float valve is completely closed.

The experiments are carried out considering the tank was completely empty in order to reproduce a typical scenario of the intermittent water supply systems. During the event of absence of service, in fact, the users collect water from the private tank that is almost empty when the service starts. During the supply period, the users collect water from the network, thus guaranteeing the private tank filling process is complete.

For each test case, seven experiments were conducted by changing the pressure from 2 to 5 bar, with a step of 0.5 bar. This pressure range ensures that the plastic pipes are not affected by deformations.

The water volume which flows into the tank was evaluated through the electromagnetic flow meter installed in the WDN (see Figure 1). The hydraulic head H used in Equation (5) to estimate Q_{up} was measured by means of a piezoresistive pressure transducer (with an accuracy of 0.1%). The data was collected with a sampling rate of 1 Hz. Each experiment was repeated twice and the average value was considered.

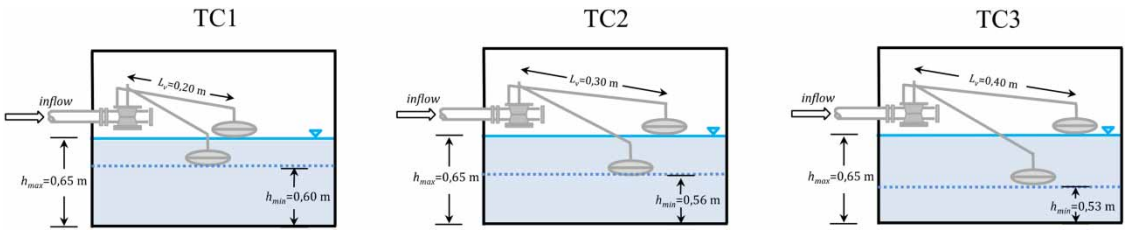

Figure 2 | Layout of the water tank and the float valve. TC1 branch of 20 cm; TC2 branch of 30 cm; TC3 branch of 40 cm.

RESULTS

The experiments were carried out with the aim of finding a mathematical model able to estimate the flow discharge into a local tank, controlled by a float valve. The experimental data were compared to the numerical data obtained including Equations (5) and (7) within the Torricelli law, repeated below:

$$Q_{up} = C_v a_v \sqrt{2g(H - z_r)}$$

The equation is governed by two coefficients, C_v and a_v. C_v is the float valve emitter coefficient; a_v is the valve discharge area. Initially, the valve discharge area was kept constant and the emitter coefficient was modelled according to a hyperbolic law, see Equation (4). At a later stage, the variation of the valve area during the opening/closing processes was taken into account, modelling its variation according to a hyperbolic law, see Equation (6).

Experiments and mathematical laws: hyperbolic law for *Cv* and constant a_v

Figure 3 compares data collected from the TC1 experiments with results obtained from the hyperbolic law given by Equation (5). Data reported hereafter have been averaged, thereby achieving one datum per minute. The pressure varies from 2 to 5 bar with a step of 0.5. Overall, as expected, the more the hydraulic head grows the more the flow rate Q increases. On the other hand, the time of the filling process becomes increasingly shorter as the pressure increases. Finally, the front of the curve, which is representative of the closure phase of the valve, progressively increases its slope. For a pressure of 5 bar, the front is almost vertical due to the rapid closure of the valve. It can be seen from Figure 3(a) ($P = 2$ bar) that the filling process is completed in approximately 45 minutes and the float valve starts to close after approximately 25 minutes, resulting in a closure period of approximately 20 minutes. On the other hand, as shown in Figure 3(g), when the network pressure is increased ($P = 5$ bar), the tank is completely filled in approximately 30 minutes.

The valve begins the closure phase after 15 minutes and the closing period continues for 17 minutes. The results reported in Figure 3(b)–3(f) behave coherently with the above description.

The comparison between the experimental data and the proposed hyperbolic laws clearly shows that although the hyperbolic law is able to reproduce the experimental data, some deviations occur during the final phase of its closure. This deviation increases with pressure, due to the more rapid closure of the valve.

Similar results can be observed for the cases TC2 and TC3, plotted in Figures 4 and 5 respectively. The comparisons between the three cases show that increasing the length of the valve branch increases the time needed to complete the tank filling. In the TC3 case, with a pressure of 2 bar (Figure 4(a)) the tank is completely filled in approximately 1 hour, whereas the valve starts to close after 28 minutes. Coherently, Figure 4(g) shows that when the network pressure is increased ($P = 5$ bar), the tank is completely filled in approximately 34 minutes. The valve begins the closure phase after 10 minutes and the closing period continues for 24 minutes. The filling process time can be a useful indicator for the water utilities to estimate the minimum time of service required to guarantee the filling of the reservoirs. Similar results are achieved in the valve branch of 30 cm (case TC2). Interestingly, when the length of the float valve is increased, the agreement between the hyperbolic law and the collected data increases. In the TC3 an almost perfect overlap between the mathematical law and the data is observed.

The best agreement between the curve obtained from Equation (5) and the experimental data was obtained calibrating the coefficient m and C_v^*. The best fitting was verified through the minimization of the root mean square error (RMSE) and the Nash–Sutcliffe model (N-S). Table 1 reports the values of the coefficients obtained for all the experiments.

In Figure 6 the variations of the coefficient m and C_v^* versus the water head are plotted. It is clear that all the values of the coefficient m have a linear trend, as clearly shown in Figure 6(a).

The line is represented by the equation:

$$m = -0.02H + 3.35 \quad (8)$$

where H is the water head. Also, in this case the values of the intercept (3.35) and of the slope (−0.02) were obtained through the minimization of the RMSE.

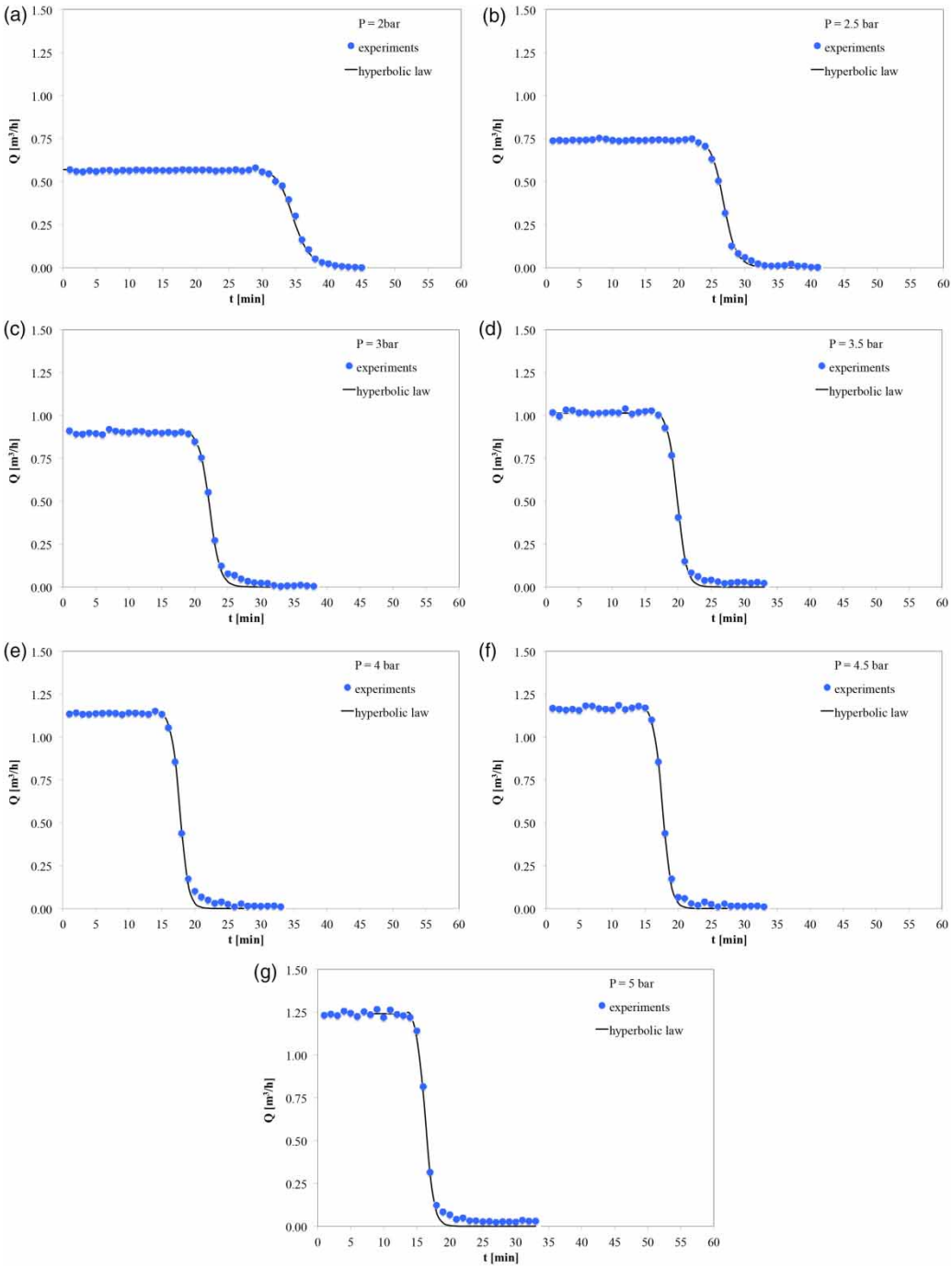

Figure 3 | TC1. Flow rate during the tank filling process, considering a constant value of a_v. Symbols: experiments; bold line: hyperbolic law. (a) Pressure 2 bar; (b) pressure 2.5 bar; (c) pressure 3 bar; (d) pressure 3.5 bar; (e) pressure 4 bar; (f) pressure 4.5 bar; (g) pressure 5 bar.

The emitter parameter C_v^* of the open valve, plotted in Figure 6, decreases with the water head depending on the increase in local head loss due to the valve, and, as reported in the preliminary research of De Marchis *et al.* (2016), the variation is not linear; in the analyzed case, it is well interpolated by the following power law:

$$C_v^* = C_{v0} + \alpha \cdot (H - H_0)^{-\beta} \tag{9}$$

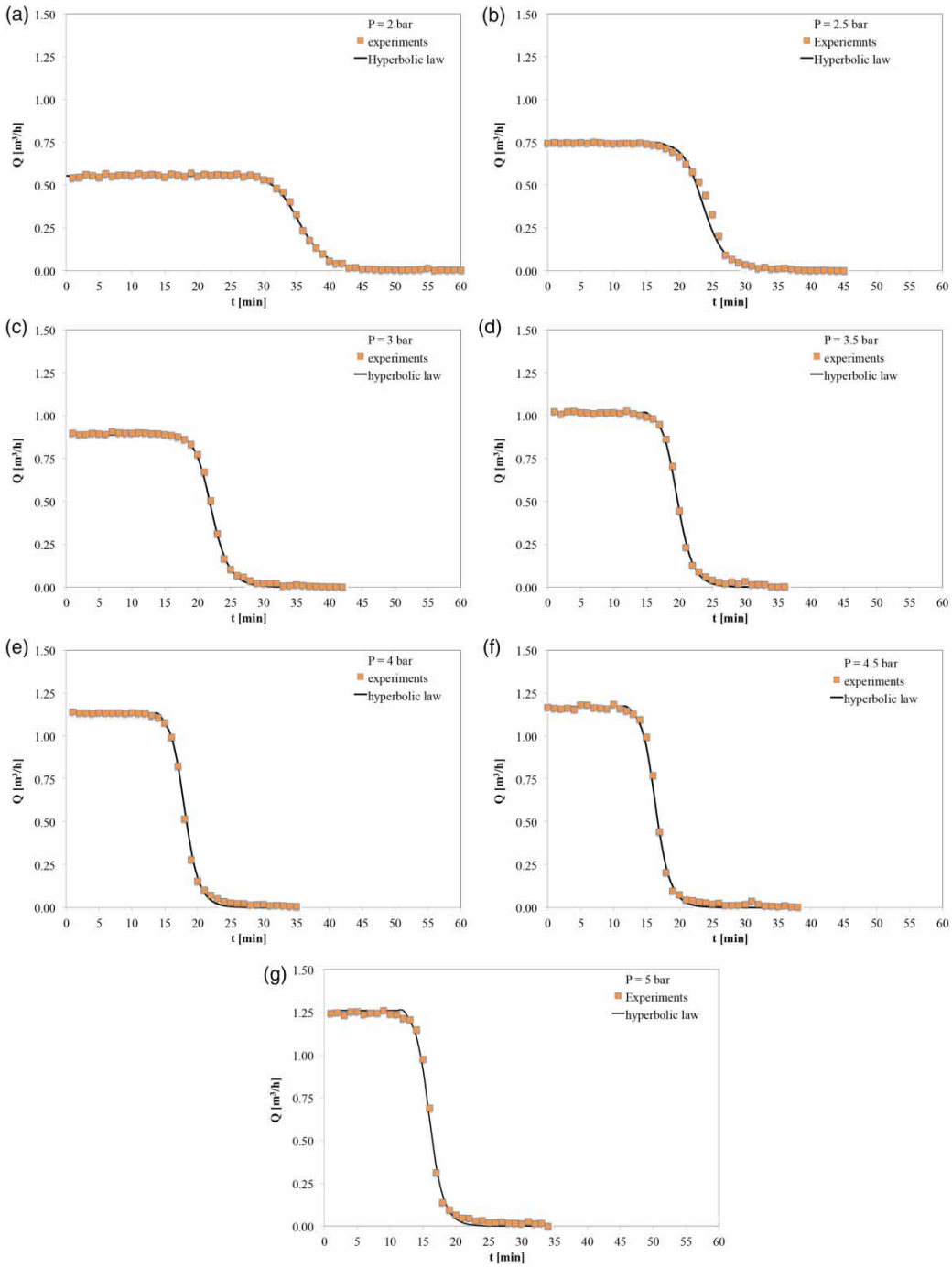

Figure 4 | TC2. Flow rate during the tank filling process, considering a constant value of a_v. Symbols: experiments; bold line: hyperbolic law. (a) Pressure 2 bar; (b) pressure 2.5 bar; (c) pressure 3 bar; (d) pressure 3.5 bar; (e) pressure 4 bar; (f) pressure 4.5 bar; (g) pressure 5 bar.

where C_{v0} is a horizontal asymptote equal to 0.30, H_0 is a vertical asymptote equal to 13, whereas the shape coefficients α and β are equal to 6 and 1.45, respectively.

Finding parametric equations that are able to reproduce physical phenomena is of fundamental importance for the development of numerical models with the ability

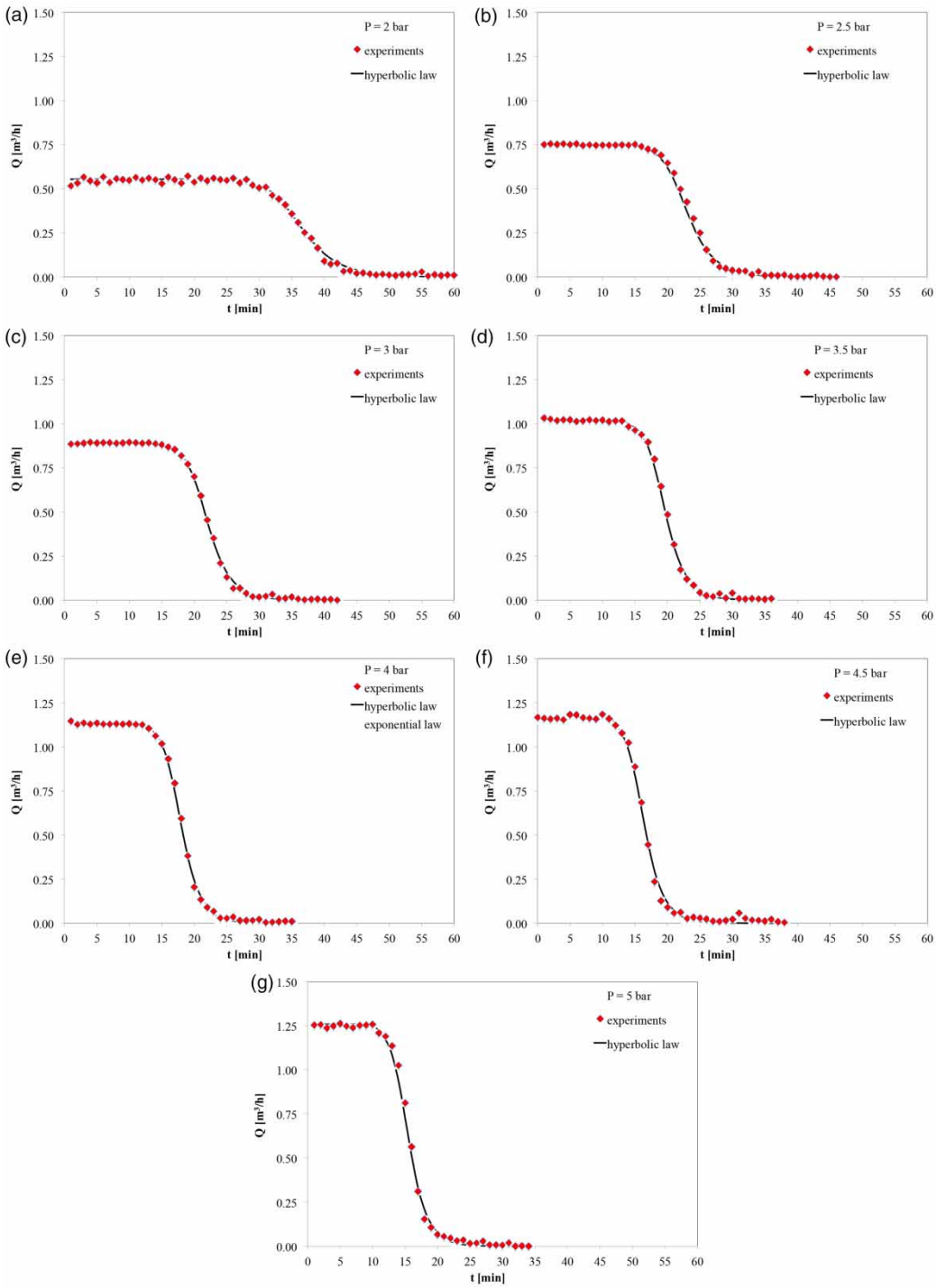

Figure 5 | TC3. Flow rate during the tank filling process, considering a constant value of a_v. Symbols: experiments; bold line: hyperbolic law. (a) Pressure 2 bar; (b) pressure 2.5 bar; (c) pressure 3 bar; (d) pressure 3.5 bar; (e) pressure 4 bar; (f) pressure 4.5 bar; (g) pressure 5 bar.

to study physical phenomena of practical interest. In this framework, the results presented show that the hyperbolic tangent law can be used in numerical codes to reproduce the WDN, in which users address water scarcity conditions through the use of local reservoirs (see De Marchis *et al.* 2011).

Table 1 | Coefficients of the float valve laws m and c_v^*

Test case	Coefficient	2 bar	2.5 bar	3 bar	3.5 bar	4 bar	4.5 bar	5 bar
TC1	m	2.72	2.60	2.52	2.37	2.30	2.20	2.10
TC2	m	2.75	2.65	2.55	2.45	2.35	2.25	2.15
TC3	m	2.78	2.55	2.50	2.43	2.37	2.23	2.15
TC1	C_v^*	0.62	0.43	0.39	0.38	0.37	0.34	0.35
TC2	C_v^*	0.62	0.43	0.38	0.37	0.36	0.33	0.33
TC3	C_v^*	0.62	0.43	0.39	0.37	0.36	0.34	0.34

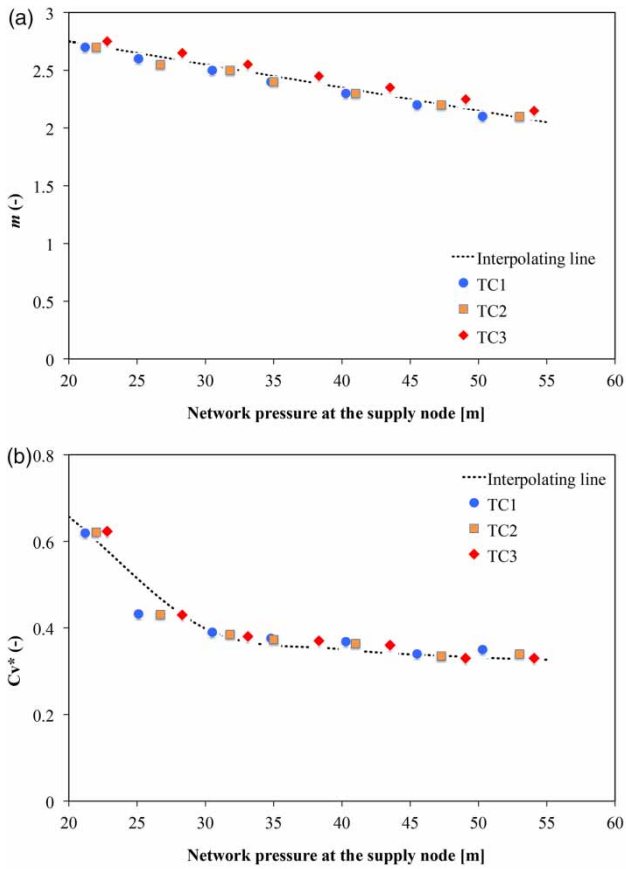

Figure 6 | Variation of the coefficients m and C_v^* with the water head H. Top panel m coefficient: Thin dotted line: Eq. m = − 0.02H +3.35. Bottom panel C_v^* coefficient: The interpolating dotted line has the Eq: $C_v^* = C_{vo} + \alpha \cdot (H - H_0)^{-\beta}$.

Experiments and mathematical laws: hyperbolic law for C_v and a_v

Even though the results above show the ability of the mathematical model to reproduce the experimental data and to capture a fast closure of the float valve, some deviations were observed when the valve closure is nearly complete, at least for the short branch; furthermore, the model needs the calibration of several coefficients (see Equations (8) and (9)). In order to improve and simplify the float valve emitter law, the model was modified taking into account a hyperbolic law to model the closure of the discharge area a_v. Basically, the discharge is calculated according to Equation (7) above.

Figures 7–9 show the comparison between the experiments and the new formulation of the float valve emitter law. Interestingly, the agreement is clearly improved when the discharge area is calculated with a hyperbolic law. The deviations initially observed for the valve branch of 20 cm disappear. Moreover the coefficients m and n have a constant value. In all the test cases and for all the pressures considered, the results presented in Figures 7–9 have been obtained by assigning $m = 2.5$ and $n = 4$. This result is clearly attractive for the development of numerical code to reproduce WDN.

In order to show the ability of the mathematical model to reproduce the experimental data, in Table 2 the achieved values of N-S coefficients are reported. All the cases are characterized by values of N-S higher than 0.99.

CONCLUSIONS

Private tanks greatly affect the hydraulic behaviour of the network. In fact, the reservoirs create a high level of supply at the beginning of the service period, reducing the pressure level on the network. Under such conditions the formulation of the specific law accounting for the existence of inline tanks must be used. The existing formulations fail during the closure phase of the float valve. Experiments have been carried out to reproduce the filling process of

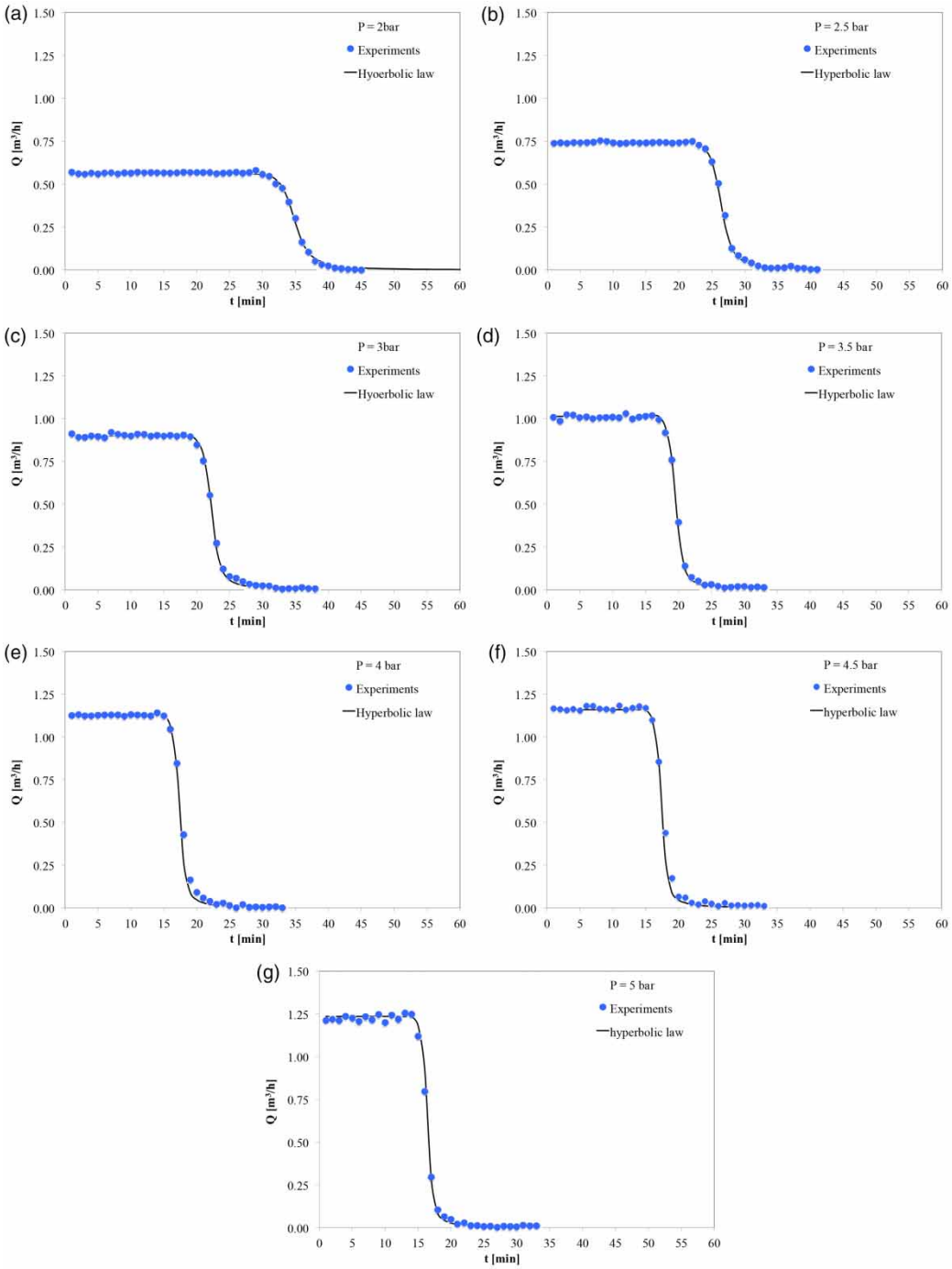

Figure 7 | TC1. Flow rate during the tank filling process, considering a hyperbolic law for a_v. Symbols: experiments; bold line: hyperbolic law. (a) Pressure 2 bar; (b) pressure 2.5 bar; (c) pressure 3 bar; (d) pressure 3.5 bar; (e) pressure 4 bar; (f) pressure 4.5 bar; (g) pressure 5 bar.

private water tanks, directly connected to the WDN. A hyperbolic tangent law is proposed for the emitter coefficient C_v and for the discharge area a_v of the head-discharge relationship. The mathematical model has been compared with existing float valve law and with laboratory experiments, carried out for different values of pressure and for three branches of different lengths. The results demonstrate the ability of the hyperbolic tangent law to

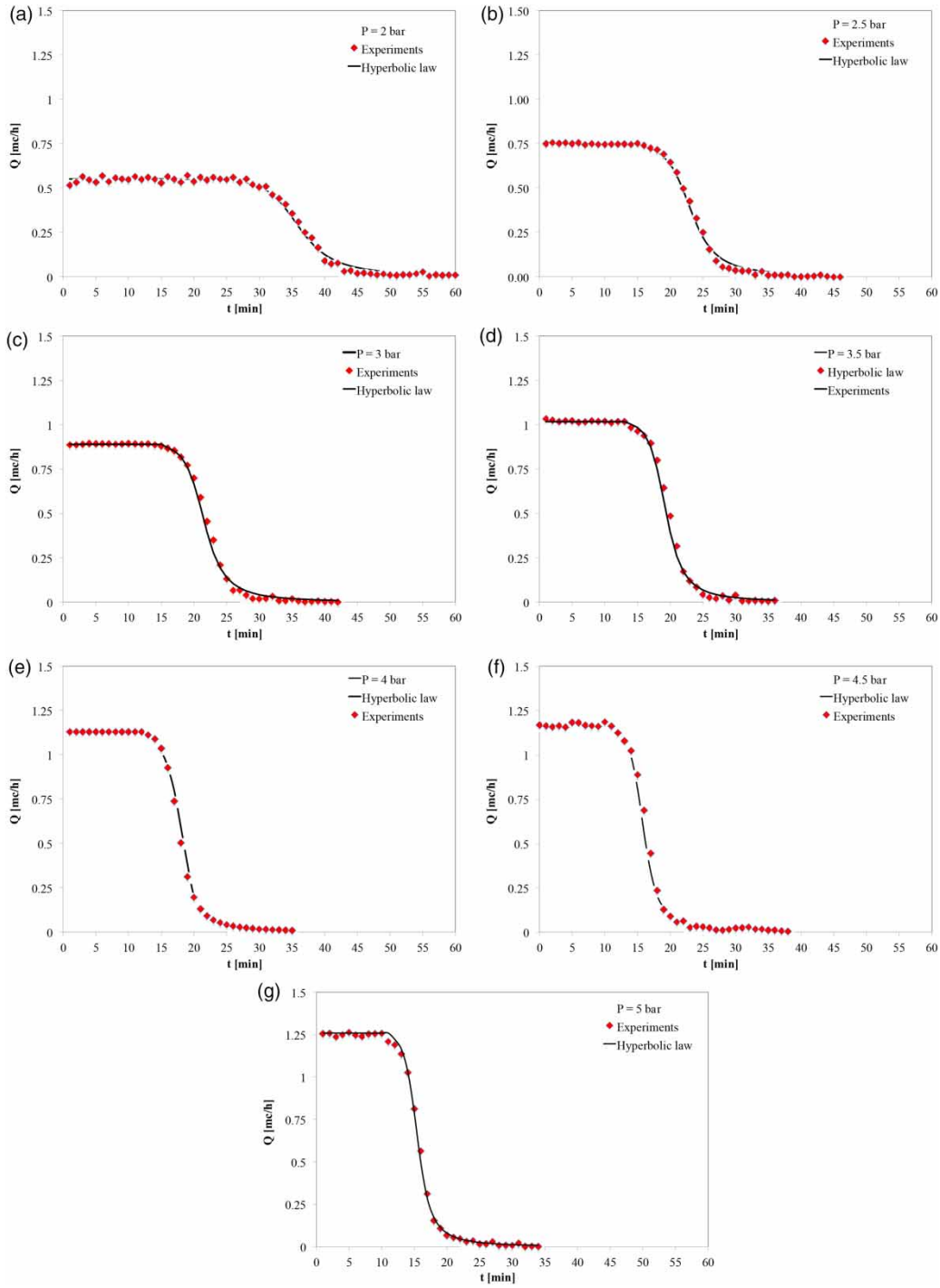

Figure 8 | TC2. Flow rate during the tank filling process, considering a hyperbolic law for a_v. Symbols: experiments; bold line: hyperbolic law. (a) Pressure 2 bar; (b) pressure 2.5 bar; (c) pressure 3 bar; (d) pressure 3.5 bar; (e) pressure 4 bar; (f) pressure 4.5 bar; (g) pressure 5 bar.

reproduce the filling process both when the valve is completely open and during the valve closure period. The mathematical system can be used in a transient model to correctly estimate the supplied demand in the presence of private tanks equipped with float valves. Further efforts are required to validate the ability of the proposed

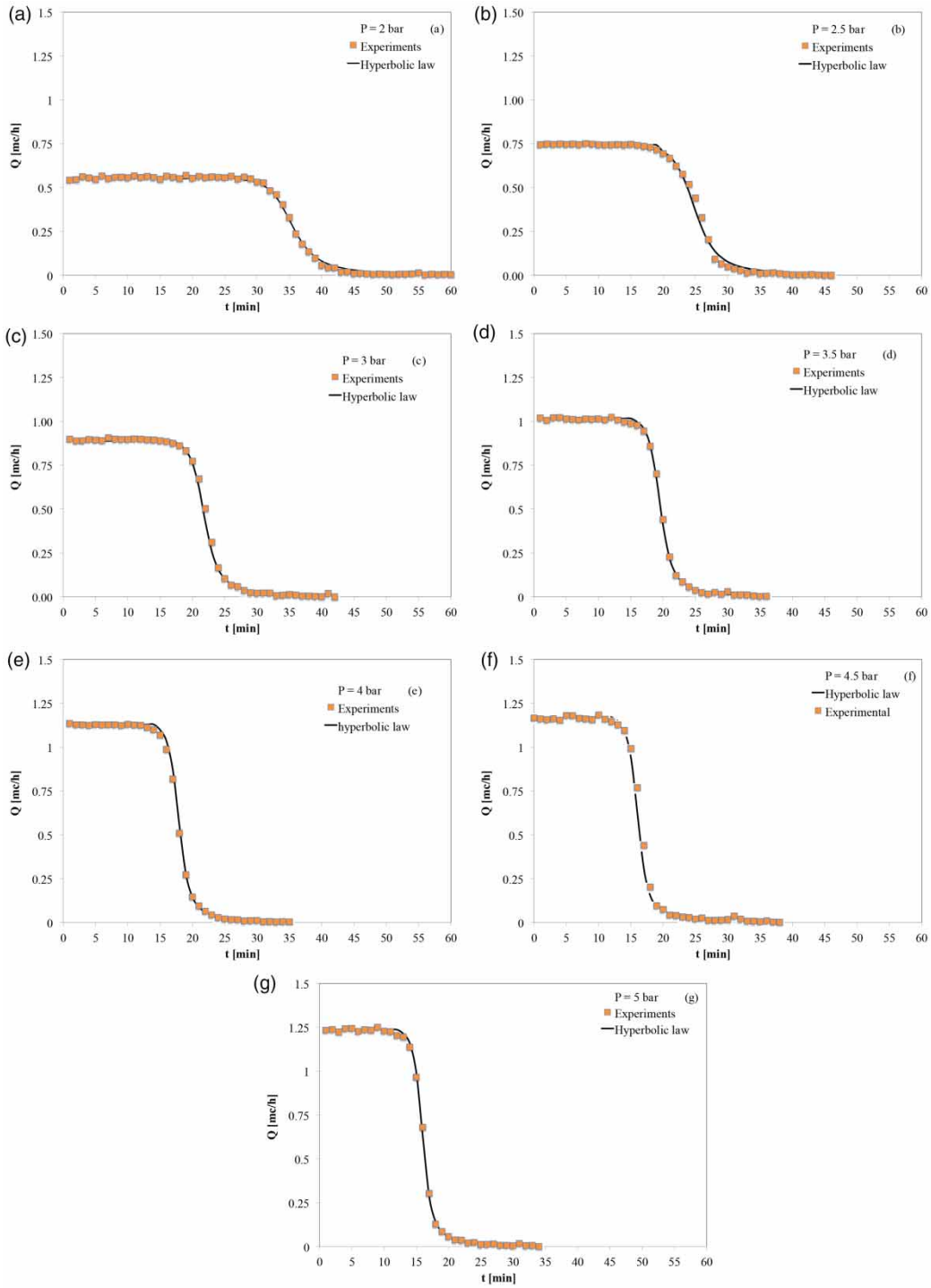

Figure 9 | TC3. Flow rate during the tank filling process, considering a hyperbolic law for a_v. Symbols: experiments; bold line: hyperbolic law. (a) Pressure 2 bar; (b) pressure 2.5 bar; (c) pressure 3 bar; (d) pressure 3.5 bar; (e) pressure 4 bar; (f) pressure 4.5 bar; (g) pressure 5 bar.

hyperbolic tangent law in pressure-driven steady state models. Moreover, new experiments are under consideration which would take into account the consumption pattern during the filling process. This way it will be possible to give more insights into the effect of the private tanks and validate the hyperbolic tangent law.

Table 2 | Average value of the Nash–Sutcliffe coefficient between experiments and mathematical values. Equation (5) is relative to the data plotted in Figures 3–5, where the float valve area is kept constant. Equation (7) is relative to the data plotted in Figures 7–9 where the float valve area is modelled through hyperbolic law

Test case	Model	2 bar	2.5 bar	3 bar	3.5 bar	4 bar	4.5 bar	5 bar
TC1	Equation (5)	0.993	0.995	0.996	0.996	0.994	0.995	0.994
TC2	Equation (5)	0.994	0.996	0.995	0.997	0.996	0.997	0.997
TC3	Equation (5)	0.995	0.996	0.997	0.997	0.998	0.998	0.998
TC1	Equation (7)	0.995	0.999	0.998	0.997	0.998	0.997	0.997
TC2	Equation (7)	0.996	0.998	0.998	0.998	0.998	0.999	0.999
TC3	Equation (7)	0.997	0.997	0.998	0.998	0.998	0.999	0.999

REFERENCES

Ackley, J. R. L., Tanyimboh, T. T., Tahar, B. & Templeman, A. B. 2001 Head-driven analysis of water distribution systems. In: *Proceedings Computing and Control for the Water Industry CCWI 2001*, Water software systems: theory and applications, Vol. 1. Research Studies Press, UK, pp. 183–192.

Bhave, P. R. 1981 Node flow analysis of water distribution systems. *J. Transp. Eng.* **107**, 457–467.

Criminisi, A., Fontanazza, C. M., Freni, G. & La Loggia, G. 2009 Evaluation of the apparent losses caused by water meter under-registration in intermittent water supply. *Water Sci. Technol.* **60** (9), 2373–2382.

De Marchis, M., Fontanazza, C. M., Freni, G., La Loggia, G., Napoli, E. & Notaro, V. 2011 Analysis of the impact of intermittent distribution by modelling the network-filling process. *J. Hydroinform.* **13** (3), 358–373.

De Marchis, M., Freni, G. & Napoli, E. 2013 Modelling of E. coli distribution in coastal areas subjected to combined sewer overflows. *Water Science & Technology* **68** (5), 1123–1136.

De Marchis, M., Milici, B. & Freni, G. 2015a Pressure-discharge law of local tanks connected to a water distribution network: experimental and mathematical results. *Water* **7**, 4701–4723.

De Marchis, M., Milici, B. & Napoli, E. 2015b Numerical observations of turbulence structure modification in channel flow over 2D and 3D rough walls. *Int. J. Heat Fluid Flow* **56**, 108–123.

De Marchis, M., Freni, G. & Milici, B. 2016 Experimental evidence of the discharge law in private tanks connected to water distribution networks. *Proc. Eng.* **154**, 115–122.

Freni, G., De Marchis, M. & Napoli, E. 2014 Implementation of pressure reduction valves in a dynamic water distribution numerical model to control the inequality in water supply. *J. Hydroinform.* **16** (1), 207–217.

Germanopoulos, G. 1985 A technical note on the inclusion of pressure dependent demand and leakage terms in water supply network models. *Civil Eng. Syst.* **2** (3), 171–179.

Giustolisi, O., Berardi, L. & Laucelli, D. 2012 Generalizing WDN simulation models to variable tank levels. *J. Hydroinform.* **14** (3), 562–573.

Giustolisi, O., Berardi, L. & Laucelli, D. 2014 Modeling local water storages delivering customer demands in WDN models. *J. Hydraul. Eng.* **140**, 89–104.

Giustolisi, O., Ugarelli, R., Berardi, L., Laucelli, D. & Simone, A. 2017 Strategies for the electric regulation of pressure control valves. *J. Hydroinform.* **19** (5), 207–217.

Gupta, R. & Bhave, P. R. 1996 Comparison of methods for predicting deficient-network performance. *J. Water Resour. Plan. Manage.* **122** (3), 214–217.

Puleo, V., Fontanazza, C. M., Notaro, V., De Marchis, M., Freni, G. & la Loggia, G. 2014 Pumps as turbines (PATs) in water distribution networks affected by intermittent service. *J. Hydroinform.* **16** (2), 259–271.

Reddy, L. S. & Elango, K. 1989 Analysis of water distribution networks with head dependent outlets. *Civil Eng. Syst.* **6** (3), 102–110.

Tabesh, M., Shirzad, A., Arefkhani, V. & Mani, A. 2014 A comparative study between the modified and available demand driven based models for head driven analysis of water distribution networks. *Urban Water J.* **11** (3), 221–230.

Tanyimboh, T. T. & Templeman, A. B. 2004 A new nodal outflow function for water distribution networks. In: *Proceedings of the 4th International Conf. on Engineering Computational Technology*. Article 64, CD-ROM. Civil-Comp Press, Stirling, Scotland.

Tanyimboh, T. T. & Templeman, A. B. 2010 Seamless pressure deficient water distribution system model. *Water Manag.* **163** (8), 389–396.

Tanyimboh, T. T., Tabesh, M. & Burrows, R. 2001 Appraisal of source head methods for calculating reliability of water distribution networks. *J. Water Res. Plan. Manag.* **127**, 206–213.

Tucciarelli, T., Criminisi, A. & Termini, D. 1999 Leak analysis in pipeline systems by means of optimal valve regulation. *J. Hydr. Eng.* **125**, 277–285.

Volpe, M., D'Anna, C., Messineo, S., Volpe, R. & Messineo, A. 2014 Sustainable production of bio-combustibles from pyrolysis of agro-industrial wastes. *Sustainability* **6** (11), 7866–7882.

First received 16 October 2017; accepted in revised form 23 February 2018. Available online 21 March 2018